Desalination and Water Treatment
www.deswater.com

doi: 10.5004/dwt.2019.24437

163 (2019) 376–384
September

Effective removal of Reactive Orange 16 dye from aqueous solution by amine-functionalized sepiolites

Slavica Lazarević[a], Vesna Marjanović[b], Ivona Janković-Častvan[a,*], Ljiljana Živković[c], Djordje Janaćković[a], Rada Petrović[a]

[a]*Faculty of Technology and Metallurgy, University of Belgrade, Karnegijeva 4, P.O. Box: 3503, 11120 Belgrade, Serbia, Tel. +381 11 3303 719; emails: icastvan@tmf.bg.ac.rs (I. Janković Častvan), slazarevic@tmf.bg.ac.rs (S. Lazarević), Tel. +381 11 3303 693; email: nht@tmf.bg.ac.rs (D. Janaćković), Tel. +381 11 3303 721; email: radaab@tmf.bg.ac.rs (R. Petrović)*
[b]*High Business-Technical School, Trg Svetog Save 34, 31000 Užice, Serbia, Tel. +381 31 512 013; email: vesnamarjanovic031@gmail.com*
[c]*Vinča Institute of Nuclear Sciences, University of Belgrade, P.O. Box: 522, 11001 Belgrade, Serbia, email: ljzivkovic@vin.bg.ac.rs*

Received 28 January 2019; Accepted 17 May 2019

ABSTRACT

Natural and acid-activated sepiolites, functionalized by covalent grafting of [3-(2-aminoethylamino) propyl]trimethoxy-silane were used as adsorbents for the removal of an anionic Reactive Orange 16 dye from aqueous solutions. The influence of initial pH (pH_i) on the adsorption was first investigated in comparison with the adsorption onto unmodified sepiolites; then the dye removal process by modified samples was subjected to kinetic and equilibrium studies at pH_i = 2.0 or 5.0, at different temperatures. Results showed that the adsorption of dye was favorable at lower pH_i and at higher temperatures, in terms of adsorption capacity and rate of adsorption. The binding sites on the adsorbents surfaces were considered to be protonated amine groups, which play a role in the electrostatic interactions with the dye anions at pH_i = 2.0. Formation of hydrogen bonds between hydrogen from amine groups and oxygen from the dye and van der Waals forces were proposed as the mechanisms of adsorption at pH_i = 5.0. The adsorption kinetics was well fitted to the pseudo-second-order kinetic model, while the equilibrium adsorption data were well correlated with the Sips isotherm. The adsorption capacity of both modified sepiolites was much higher than of the parent samples, whereas the capacity of the functionalized acid-activated sepiolite was higher (~172 mg/g) than of the functionalized natural sepiolite (~158 mg/g) at 298 K, pH_i 5.0.

Keywords: Sepiolite; Functionalization; Adsorption; Reactive Orange 16; Kinetics

1. Introduction

Organic synthetic dyes (OSD) are widely used to modify the color characteristics of different substrates, including paper, leather, fur, plastics and textile. Accompanying their large-scale production and extensive applications, OSD can cause environmental pollution and affect human health. The presence of OSD in the water bodies increases the chemical oxygen demand as well as adversely influences the metabolism of aquatic organisms. In addition, OSD are serious human health-risk factor, because they can cause dysfunction of kidneys, reproductive system, liver, brain and central nervous system [1,2]. Therefore, to protect environment and human health, it is necessary to regulate the concentration of OSD in waste effluents before they are discharged into the environment.

Reactive OSD are extensively used in the textile industry, due to their superior dyeing properties, especially in terms of fastness. They differ from other classes of OSD in that they bind to textile fibers by covalent bonds. Since reactive OSD

* Corresponding author.

1944-3994/1944-3986 © 2019 Desalination Publications. All rights reserved.

usually present high stability under sunlight and resistance to microbial attack and temperature, the large majority of these compounds are not degradable in conventional wastewater treatment plants [3–5]. Among different technologies utilized for the removal of these pollutants, oxidation and adsorption are the most promising [1,2,4]. Oxidation methods are probably the best technologies to eliminate organic carbon, but OSD are generally very resistant to common oxidation agents and complete mineralization is difficult to achieve [4,6]. Although the oxidation processes have been improved by simultaneous use of more than one oxidant (advanced oxidation processes) [7–9], these technologies are not completely accepted at present because they are quite expensive and have operational problems. In addition, the likelihood of OSD being completely mineralized to CO_2 and H_2O is still low and some undesirable by-products are usually formed.

By proper selection of the adsorbent, the adsorption can be a simple, environmentally friendly and low cost operation of high efficiency, without producing undesirable by-products [6,10,11]. Various waste materials and natural minerals, which are cheap and can be used as such or after some minor treatment, have been extensively searched and tested for OSD adsorption [1,2,6,10]. Clay-based adsorbents are promising adsorbents for the removal of OSD [12,13], but mainly for cationic types, while anionic ones are not adsorbed well due to the negatively charged surface. Sepiolite, a fibrous clay mineral of high specific surface area, is also a very good adsorbent for cationic OSD [14–20], but its adsorption capacity for anionic OSD is very low [21–27], as in the case of other clay minerals. In order to increase the adsorption capacity, sepiolite has been modified by acid activation [28], thermal treatment [23,28], formation of nanohybrides [29], surface modifications [30–33], etc. It was shown that affinity for anions could be highly improved by functionalization of sepiolite surface with silane reagents [32–35]. In addition, the adsorption capacity was increased by sepiolite acid-activation followed by functionalization [34,35]. In all cases, adsorption was favored at lower pH values, owing to positive surface charge of adsorbents.

Therefore, in this work, the efficiency of functionalized natural and acid-activated sepiolite for the removal of anionic dye Reactive Orange 16 from water was studied, keeping in view its widespread use in industries and thereby high probability of its release into the wastewater. Natural and acid-activated sepiolites were functionalized with [3-(2-aminoethylamino) propyl]trimethoxy-silane and batch adsorption experiments were conducted to investigate and compare their adsorption behaviors with the parent samples. The effects of initial solution pH, initial dye concentration, contact time and temperature on the adsorption process were studied. The capabilities of the Langmuir, Freundlich and Sips isotherm models to fit the equilibrium adsorption data were investigated, while the pseudo-first, pseudo-second-order and intra-particle diffusion models were used to fit the kinetic adsorption data.

2. Materials and methods

2.1. Materials

The natural sepiolite (SEP) from Andrići (Serbia) was used as a starting material, of which the particles under 250 μm were used in experiments. The acid-activated sample (ASEP) was prepared by stirring of the dispersion of 10 g of SEP in 100 cm^3 of 4 M HCl solution for 10 h at room temperature, followed by centrifugation and washing with distilled water. The obtained acid-activated sample was dried at 110°C for 2 h [36].

Natural and acid-activated sepiolites were functionalized with [3-(2-aminoethylamino) propyl]trimethoxy-silane or amine-silane, APT ($(CH_3O)_3Si–(CH_2)_3–NH–(CH_2)_2–NH_2$, Sigma-Aldrich, USA) [35]. A mixture of 10 g of SEP or ASEP and 100 cm^3 of toluene was refluxed and mechanically stirred for 1 h under dry nitrogen. Then, 5 cm^3 of amine-silane was added dropwise and the mixture was refluxed for 24 h, filtered, and washed with water, then by methanol and acetone. So-obtained functionalized sepiolites, APT-SEP and APT-ASEP, were dried under dry nitrogen for 24 h. The physico-chemical properties of the samples were reported previously [35].

The dye solutions used in the experiments were prepared by dissolving the required amount of Reactive Orange 16 dye (RO 16) of analytical grade in distilled water. The structure of RO 16 dye is shown in Fig. 1.

2.2. Adsorption experiments

All adsorption experiments were carried out using the batch method, at a ratio adsorbent to dye solution of 0.04 g: 20 cm^3. The suspensions were equilibrated at a constant temperature in the thermostatic shaker (MEMMERT, Germany). After adsorption, the suspensions were centrifuged and the final solution pH values were determined. The concentration of RO 16 in solutions before and after adsorption was determined by UV-Vis spectrophotometer (Shimadzu UV-1800, Japan). All adsorption studies were repeated twice; the reported values are the average of two measurements.

The effect of solution pH on RO 16 adsorption onto sepiolite samples was investigated at temperature 298 K with RO 16 solution of 100 mg/dm^3 concentration, by varying the initial solution pH (pH_i) from 2.0 to 5.0. Equilibration was carried out for 24 h. Solution of HCl or KOH of 0.1 mol/dm^3 concentration was used for pH adjustments.

The adsorption kinetics were investigated at 298 and 323 K at initial pH values of 2.0 and 5.0 by varying the contact time from 20 min to 24 h. RO 16 solution of initial concentrations of 200 mg/dm^3 was used.

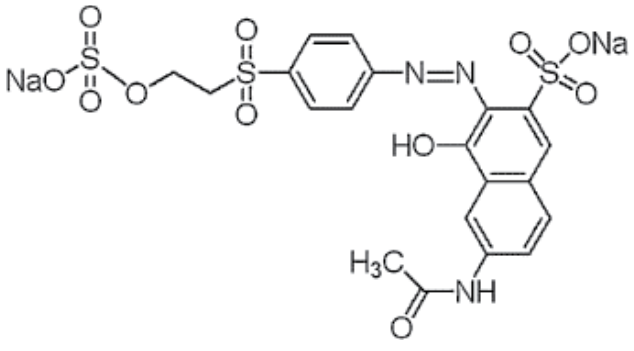

Fig. 1. Chemical structure of Reactive Orange 16.

Adsorption isotherms were determined at pH_i of 2.0 and 5.0 using RO 16 solutions of initial concentrations of 20–500 mg/dm^3, at 298, 313, 323 and 333 K. Equilibration was carried out for 24 h.

The amounts of RO 16 adsorbed per unit mass of adsorbents were calculated using Eq. (1):

$$q_e = \frac{c_i - c_f}{m} \times V \quad (1)$$

3. Results and discussion

3.1. Influence of initial pH

Fig. 2 shows the dependences of the adsorbed amount of RO 16 onto natural (SEP), acid-activated (ASEP), and functionalized sepiolites (APT-SEP and APT-ASEP) on the initial solution pH value (pH_i). These pH_i values were chosen taking into account values of point of zero charge (pH_{PZC}) of the adsorbents [35,36] and solubility of the sepiolite [36]: surface charge increase, and solubility of sepiolite also increase as the solution pH decrease.

As seen, the RO 16 adsorption increased with pH_i decreasing from 5.0 to 2.0 for all investigated sepiolite samples. According to Fig. 2, the adsorption capacity of SEP and ASEP was almost equal to 0 at pH of 4–5 and slightly higher at pH_i ~3 (3.9 mg/g SEP, 3.6 mg/g ASEP) and at pH_i ~2 (5.9 mg/g SEP, 4.3 mg/g ASEP). The adsorption capacity of both functionalized sepiolites was much higher than of natural and acid-activated sepiolites.

Adsorption of OSD onto clay adsorbents is primarily controlled by surface charge of the clay and the structure of OSD. In aqueous solution, the RO 16 dye dissociates to Na^+ and D-$(SO_3^-)_2$, and the dye anions can be removed from solution by electrostatic attraction with positive surface of adsorbent [1,3,12,13,32–36]. This anion is present in solution in wide range of pH values, even at very low pH values.

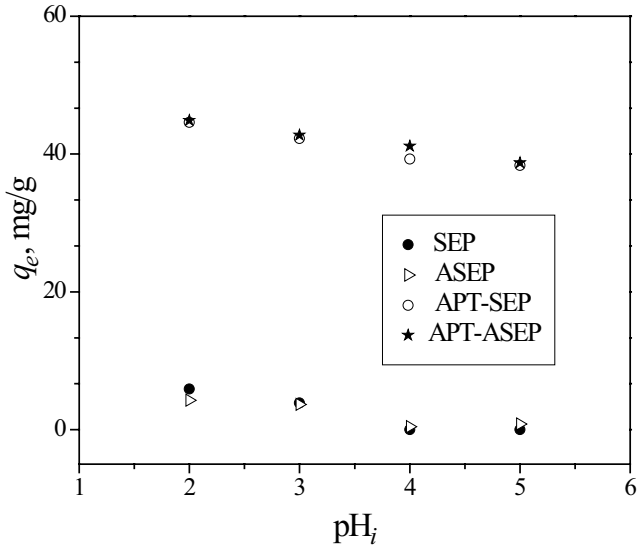

Fig. 2. Effect of pH_i of the solution on the adsorption of RO 16 onto sepiolite samples, at 298 K (c_i (RO 16) = 100 mg/dm^3).

Anions with the general formula RSO_3^- (sulfonates) are the conjugate bases of sulfonic acids (RSO_2OH), which tend to be strong acids. Therefore, the corresponding sulfonates are weak bases and protonization of SO_3^- groups is hardly to occur even at low pH values (pH 2).

The surface charge of adsorbent is governed by protonization or deprotonization of the surface functional groups: surface charge is positive at pH lower than point of zero charge (pH_{PZC}) and negative at pH > pH_{PZC}. During experiments with all sepiolite samples, at pH_i values of 5.0 and 4.0, a remarkable increase in the solution pH was observed; the equilibrium pH values were equal to pH_{PZC} of the adsorbents (~7.4 for SEP, ~6.9 for ASEP, ~10.0 for APT-SEP and ~9.9 for APT-ASEP) [35,36]. On the contrary, a small increase in the solution pH values was observed for pH_i = 2.0: the final pH values (pH_f) were around 2.2 for all samples. In the case of pH_i = 3.0, pH_f values were slightly bellow pH_{PZC} of the adsorbents: ~7.1 for SEP, ~6.5 for ASEP, ~8.6 for APT-SEP and ~8.3 for APT-ASEP. Taking into account such pH changes during adsorption, it can be stated that adsorbents surfaces had the highest positive charge at pH_i = 2.0, lower at pH_i = 3.0, while at pH_i values of 5.0 and 4.0, the surfaces of the adsorbents were not positively charged. Consequently, the highest adsorption capacity of all the adsorbents was achieved at pH_i = 2.0, as in the case of chromate anions adsorption [35]. Although the surfaces of SEP and ASEP were positively charged at pH_i = 2.0 and 3.0, the adsorption capacities were much lower than of APT-SEP and APT-ASEP. Obviously, the surface charges of functional samples were much higher, owing to high number of protonated amine groups (–NH_2^+– and –NH_3^+). Because the surfaces of SEP and ASEP were not positively charged at pH_i = 4.0 and 5.0, the adsorption capacities of these adsorbents were very low. On the other hand, high adsorption capacities of both functionalized sepiolites (about 38 mg/g) at initial solution pH values of 4.0 and 5.0, could be due to van der Waals forces and hydrogen bonding [3] between D-$(SO_3^-)_2$ and amine-silane chain grafted on the sepiolite surface.

In order to elucidate the mechanism of adsorption of RO 16 onto the functionalized sepiolites, the kinetic studies and the equilibrium adsorption experiments at different temperatures were performed at pH_i values of 2.0 and 5.0. Nonfunctionalized sepiolite samples SEP and ASEP were not considered for further study, due to low adsorption capacity.

3.2. Adsorption kinetics

The influence of contact time on RO 16 adsorption onto APT-SEP and APT-ASEP at pH_i = 2.0 and 5.0, at temperatures of 298 and 323 K, is shown in Fig. 3.

For investigated conditions of pH and temperature, the RO 16 removal by APT-SEP and APT-ASEP increased rather sharply during the first 1 h, owing to a high number of active sites available at the beginning of the adsorption. After that, a slow increase of the adsorbed amount is observed, since the greatest number of adsorption sites was occupied and the dye concentration in the solutions decreased. In addition, intra-particle diffusion of dye anion through the pores of adsorbent can be the reason for the adsorption slowdown.

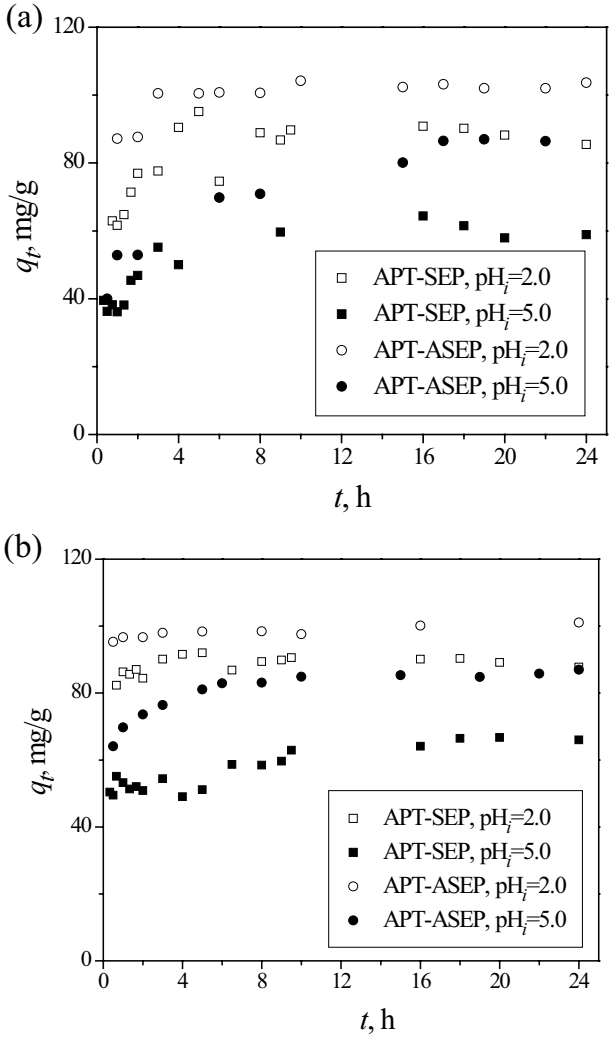

Fig. 3. Effect of contact time t on the adsorbed amount of RO 16 onto APT-SEP and APT-ASEP (c_i (RO 16) = 200 mg/dm^3) at: (a) T = 298 K and (b) T = 323 K.

The approximate contact time required to achieve equilibrium for both functionalized sepiolites decreased with temperature (Fig. 3): 4 h at 298 K and 2 h at 323 K (pH$_i$ 2.0), and 16 h at 298 K and 10 h at 323 K (pH$_i$ 5.0).

Moreover, it is obvious that the adsorption capacity of APT-ASEP was higher than of APT-SEP at both temperatures and at both pH$_i$ values. Similar as in the case of chromate adsorption [35], better amine-functionalization of the acid-activated sepiolite compared with the natural sepiolite, provided higher number of amine groups and consequently higher adsorption capacity of APT-ASEP compared with APT-SEP.

Kinetic experiments confirmed that adsorption capacities of both functionalized sepiolites were higher at pH$_i$ = 2.0 than at pH$_i$ = 5.0, at both studied temperatures and this difference was more pronounced for APT-SEP due to its lower adsorption capacity. On the other hand, it appeared that the adsorption capacity was not affected by temperature. Thus, the influence of temperature on the adsorption capacity was checked further in the study by constructing the adsorption isotherms at different temperatures.

The kinetics of RO 16 adsorption onto APT-SEP and APT-ASEP was investigated with pseudo-first-order model, by using Lagergren [37] and Annadurai/Krishnan [38] equations, the intra-particle diffusion model [39] and pseudo-second-order model [40].

The pseudo-second-order model fitted the experimental data obtained at all investigated conditions much better than pseudo-first-order models, with correlation coefficients R^2 higher than 0.99 (Table 1). Additionally, the calculated amount of dye adsorbed at equilibrium, q_e, was very close to the experimentally obtained value (Table 1; Fig. 3), which further verified the adequacy of pseudo-second-order model. This model is based on the assumption that chemisorption may be a rate-limiting step involving valence forces through share or exchange of electrons between adsorbent and adsorbate [40]. According to literature, the pseudo-second-order kinetic model is appropriate for most experimental data for adsorption of dyes on various clay materials [2,12], including sepiolite samples [24,25,30,31,41].

As seen in Table 1, the values of pseudo-second-order rate constant, k_2, and the initial adsorption rate, h, were higher at pH$_i$ = 2.0 than at pH$_i$ = 5.0, at both studied temperatures, on both adsorbents, indicating higher affinity of the adsorbents for RO 16 at pH$_i$ = 2.0 than at pH$_i$ = 5.0.

The overall rate of adsorption is controlled by the slowest step in the adsorption process: external film (boundary layer) diffusion, internal particle (intra-particle) diffusion, or adsorption. The third step is assumed rapid and, thus the slowest step would be either film diffusion or intra-particle diffusion. The intra-particle diffusion model was used to determine which step in the studied adsorption process of RO 16 was the slowest. According to this model, if intra-particle diffusion participates in the adsorption process as the sole rate-limiting step, a plot of q_t against $t^{1/2}$ should be linear and passing through the origin. On the other hand, if the dependence is linear, but does not pass through the origin, then intra-particle diffusion is involved in the adsorption process, but it is not rate-limiting step. Generally, the intercept I (Table 1) of the linear dependence on q_t axes gives an idea about boundary layer thickness: the larger the value of the intercept, the greater the boundary layer diffusion effect [39,42]. Fig. 4 shows that the dependences q_t vs. $t^{1/2}$ were generally consisted of two linear portions, where the first indicates intra-particle diffusion and the second, parallel to $t^{1/2}$ axes, indicates equilibrium. The first linear part of the dependences do not pass through the origin, indicating that intra-particle diffusion was involved in the adsorption of RO 16 onto APT-SEP and APT-ASEP, but not as the rate-controlling step. Therefore, it can be supposed that functionalization of sepiolite and acid-activated sepiolite was achieved mostly on the surface of the bundles-like aggregates formed by the surface interaction between the individual needle-type particles [43].

3.3. Adsorption isotherms at different temperatures and modeling of equilibrium data

The adsorption isotherms at different temperatures are presented in Fig. 5 for APT-SEP and Fig. 6 for APT-ASEP.

Table 1
Kinetic parameters and correlation coefficients for RO 16 adsorption by APT-SEP and APT-ASEP at 298 and 323 K, at pH_i values of 2.0 and 5.0, for c_i (RO 16) = 200 mg/dm^3 (the adsorbent to RO 16 solution ratio was 0.04 g: 20 cm^3)

Adsorbent	T (K)	pH_i	Pseudo-first-order						Pseudo-second-order			Intra-particle diffusion		
			Lagergren equation $\log(q_e - q_t) = \log q_e - \frac{k_1}{2.303}t$			Annadurai and Krishnan equation $\frac{1}{q_t} = \frac{1}{q_e} + \frac{k_1}{q_e}\times\frac{1}{t}$			$\frac{t}{q_t} = \frac{1}{k_2 q_e^2} + \frac{1}{q_e}\times t$ $h = k_2 q_e^2$			$q_t = I + k_d t^{1/2}$		
			k_1	q_e	R^2	k_1	q_e	R^2	k_2	q_e	h	R^2	k_d	I	R^2
			1/min	mg/g		1/min	mg/g		g/(mg min)	mg/g	mg/(g min)		mg/(g min$^{1/2}$)	mg/g	
APT-SEP	298	2.0	10.80×10^{-4}	19.350	0.398	25.606	95.251	0.867	9.17×10^{-4}	89.206	7.296	0.998	3.250	38.31	0.948
		5.0	13.18×10^{-4}	21.701	0.680	13.036	54.466	0.546	5.63×10^{-4}	61.425	2.124	0.997	1.135	32.15	0.850
	323	2.0	8.55×10^{-4}	4.160	0.107	4.427	90.909	0.713	79.63×10^{-4}	90.009	64.516	0.999	0.842	77.88	0.803
		5.0	26.48×10^{-4}	20.441	0.819	4.857	58.720	0.289	3.73×10^{-4}	67.385	1.693	0.996	0.546	46.81	0.744
APT-ASEP	298	2.0	16.97×10^{-4}	9.511	0.674	13.047	104.058	0.802	8.60×10^{-4}	103.734	9.251	0.999	1.001	80.93	0.707
		5.0	35.93×10^{-4}	56.160	0.856	32.273	80.645	0.891	1.43×10^{-4}	90.662	1.179	0.994	1.550	36.59	0.951
	323	2.0	15.29×10^{-4}	5.131	0.746	1.348	99.108	0.580	13.81×10^{-4}	101.010	14.100	0.999	0.151	95.18	0.846
		5.0	20.74×10^{-4}	14.118	0.818	10.779	84.674	0.903	5.75×10^{-4}	87.260	4.377	0.999	1.060	61.03	0.934

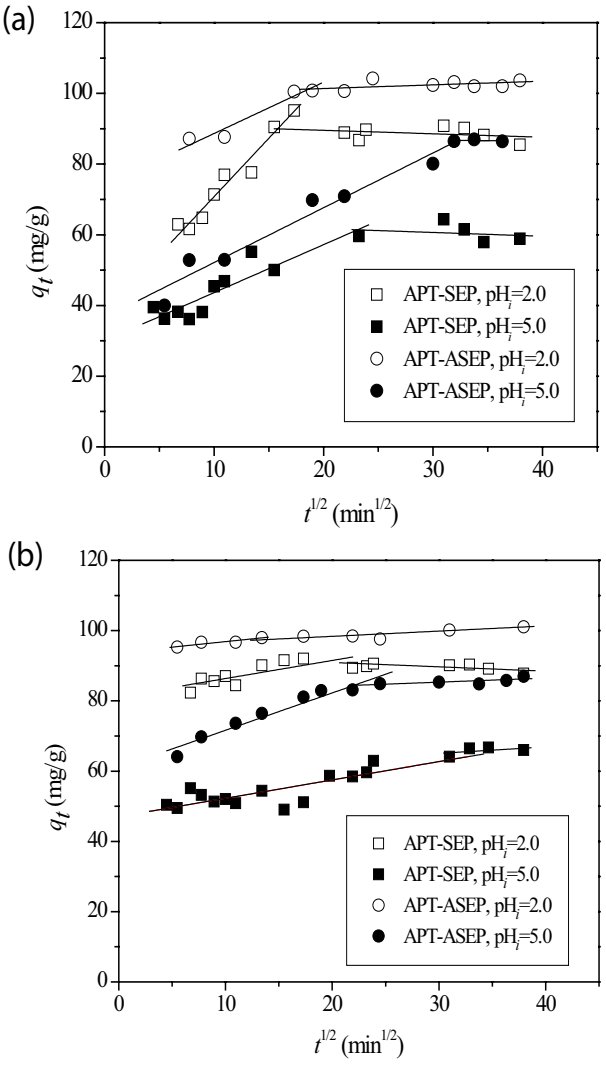

Fig. 4. Dependences q_t vs. $t^{1/2}$ for RO 16 adsorption onto APT-SEP and APT-ASEP (c_i (RO 16) = 200 mg/dm^3) at: (a) T = 298 K and (b) T = 323 K.

The equilibrium adsorption data were fitted to the Langmuir, Freundlich and Sips isotherms and the adsorption isotherms constants, determined by non-linear regression analysis using the Easy Plot, are summarized in Table 2. As an example, the models' fits are presented in Fig. 7 for both samples and both pH_i values at temperature 298 K.

The experimental data were better fitted with the Langmuir and Sips isotherms than with the Freundlich isotherm, while the Sips model was the most suitable (Table 2). The Langmuir model [44,45] assumes monolayer adsorption at specific homogeneous sites, without any interactions between adsorbed species, which are strongly attracted to the surface. On the other hand, the Freundlich equation [45,46] describes adsorption (possibly multilayer) on a heterogeneous surface consisting of energetically non-uniform sites. Sip's equation [45,47] simulates both Langmuir and Freundlich behaviors: at low adsorbate concentrations, the model reduces to Freundlich isotherm, while at high concentrations, when the adsorbate content is higher than

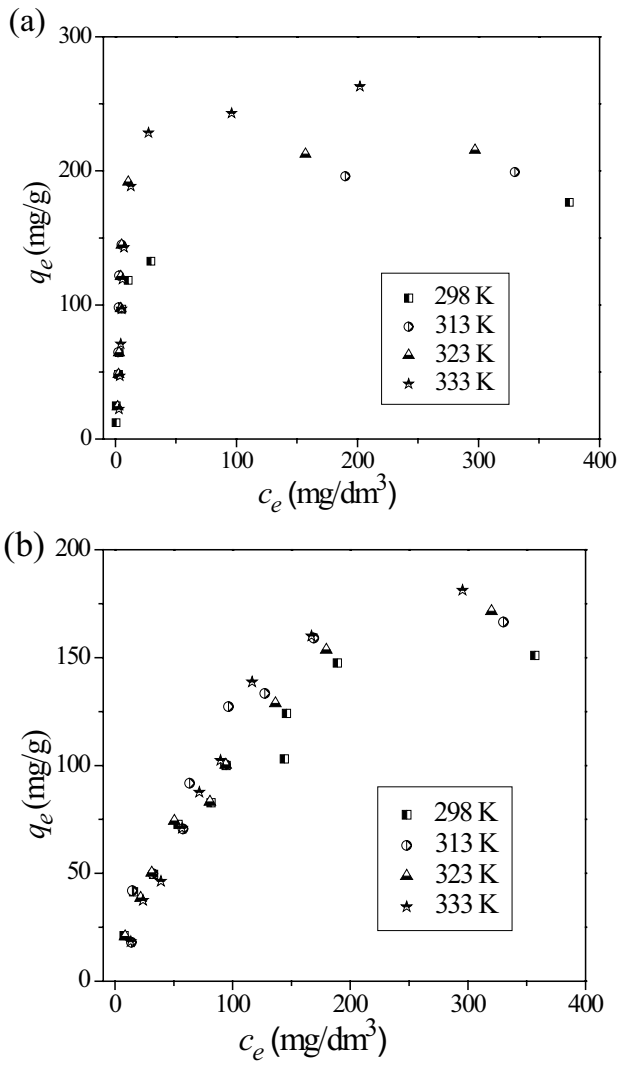

Fig. 5. Adsorption isotherms of RO 16 onto APT-SEP at different temperatures at pH$_i$ 2.0 (a) and 5.0 (b).

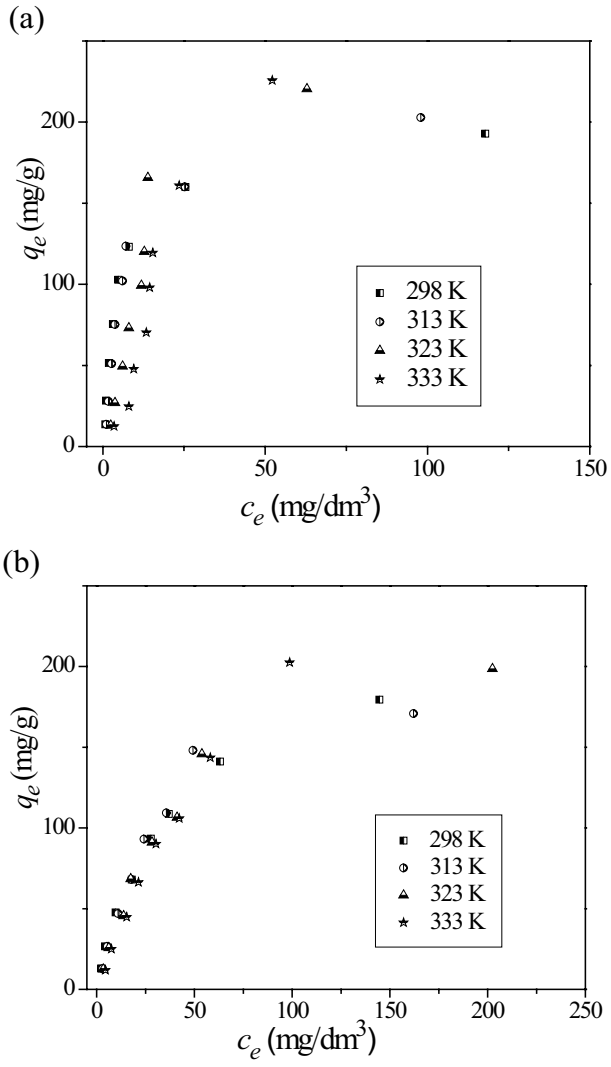

Fig. 6. Adsorption isotherms of RO 16 onto APT-ASEP at different temperatures at pH$_i$ 2.0 (a) and 5.0 (b).

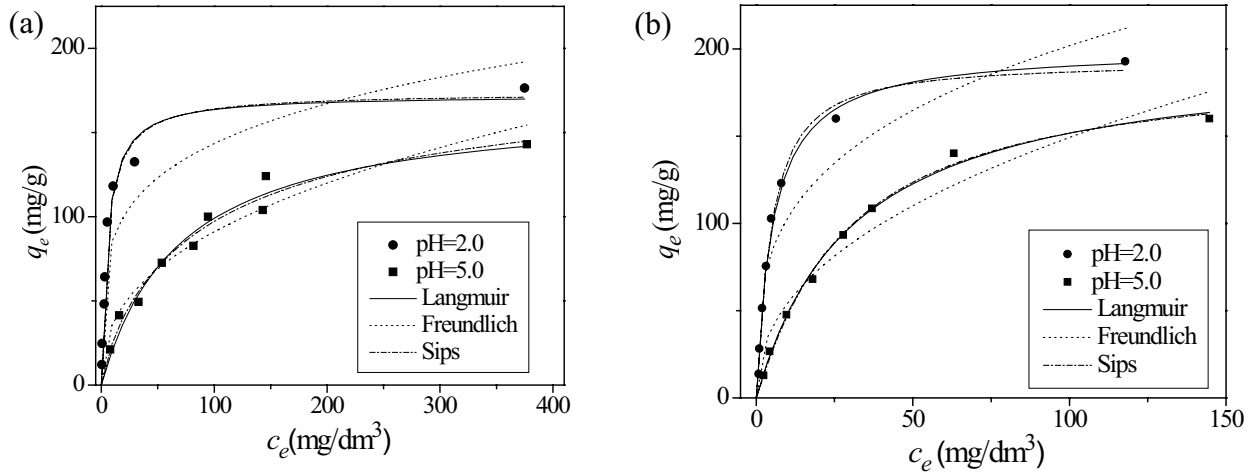

Fig. 7. Fitting of the equilibrium adsorption data at temperature 298 K to the Langmuir, Freundlich and Sips isotherms: (a) APT-SEP and (b) APT-ASEP.

Table 2
Langmuir, Freundlich and Sips parameters and correlation coefficients for RO 16 adsorption onto APT-SEP and APT-ASEP at pH_i values of 2.0 and 5.0, at various temperatures

Adsorbent	pH_i	T (K)	Langmuir isotherm $q_e = \frac{q_m K_L c_e}{1 + K_L c_e}$			Freundlich isotherm $q_e = K_f \times c_e^{1/n}$			Sips isotherm $q_e = \frac{q_m K_a (c_e)^{n_S}}{1 + K_a (c_e)^{n_S}}$			
			q_m	K_L	R^2	$1/n$	K_f	R^2	q_m	K_a	n_s	R^2
APT-SEP	2.0	298	172.2	0.190	0.984	0.22	52.0	0.859	173.4	0.196	0.963	0.984
		313	203.4	0.097	0.922	0.166	79.5	0.855	195.0	0.112	2.75	0.972
		323	236.9	0.082	0.887	0.200	73.9	0.685	213.4	0.065	2.59	0.989
		333	280.0	0.042	0.913	0.274	68.1	0.806	267.6	0.051	1.53	0.929
	5.0	298	168.0	0.082	0.980	0.340	14.5	0.957	157.6	0.070	0.830	0.980
		313	177.1	0.031	0.976	0.557	86.5	0.959	167.8	0.021	1.01	0.976
		323	184.3	0.022	0.989	0.522	9.08	0.974	175.7	0.015	0.923	0.989
		333	195.9	0.008	0.965	0.520	9.36	0.911	190.7	0.007	0.159	0.982
APT-ASEP	2.0	298	200.0	0.189	0.993	0.292	52.4	0.889	192.1	0.170	1.14	0.994
		313	218.2	0.131	0.979	0.341	45.9	0.888	212.3	0.088	1.40	0.987
		323	268.3	0.052	0.865	0.524	26.8	0.863	253.8	0.036	2.09	0.970
		333	290.6	0.013	0.941	0.782	108.4	0.919	286.9	0.017	2.56	0.987
	5.0	298	183.0	0.062	0.996	0.438	19.8	0.954	172.2	0.059	1.06	0.996
		313	198.7	0.030	0.980	0.433	208.3	0.900	187.1	0.019	1.37	0.990
		323	210.2	0.019	0.989	0.468	17.6	0.941	217.6	0.012	1.19	0.991
		333	221.0	0.007	0.998	0.767	6.08	0.990	228.9	0.007	1.00	0.998

the adsorbent capacity, it predicts a monolayer adsorption capacity, characteristic of the Langmuir isotherm.

The results presented in Figs. 5–7 and Table 2 show that the adsorption capacity of:

- both adsorbents is higher at pH_i = 2.0 than at pH_i = 5.0 at all studied temperatures
- APT-ASEP is higher than of APT-SEP at both pH_i values and at all temperatures
- both adsorbents increases with temperature at both pH_i values

An increase of the adsorption capacity with increasing temperature indicates the endothermic nature of adsorption. Generally, an exothermic adsorption process signifies either physisorption or chemisorption, but endothermic process is attributable unequivocally to chemisorption [48], that is, to the formation of strong bonds between adsorbent and adsorbate. The strength of adsorbate–adsorbent bonds in the case of studied adsorption of RO 16, can be assessed according to the value of the Sips equilibrium constant K_a: higher value of K_a implies stronger bonds between adsorbate species and adsorbent active sites. Decreasing of K_a with temperature (Table 2) indicates that bond strengths are decreased as the temperature increased, which was expected. Obviously, stronger bonds are formed at pH_i = 2.0 than at pH_i = 5.0 (Table 2), which can be also concluded according to the shape of the adsorption isotherms (Fig. 7). As assumed earlier in the text, strong electrostatic interactions between protonated amine groups and dye anions are dominant at pH_i = 2.0, while the formation of weak hydrogen bonds between hydrogen from amine groups and oxygen from the dye is the likely mechanism of adsorption at pH_i = 5.0.

4. Conclusions

The adsorption of the anionic dye Reactive Orange 16 from aqueous solutions on the amine-silane functionalized natural and acid-activated sepiolites, was investigated at various initial pH values and temperatures. In all cases, the adsorption capacity of functionalized acid-activated sepiolite was higher than of the functionalized natural sepiolite, while the capacity of both modified sepiolites was much higher than of the parent samples. Obviously, a combination of acid-activation of sepiolite, which increases the specific surface area, and functionalization, which grafts appropriate functional groups on the surface, provides the highest adsorption capacity for dye anions.

The adsorption on both functionalized sepiolites, at all temperatures, is favored at lower initial pH (2.0) via electrostatic interactions between dye anions and protonated amine groups on the adsorbents surface. High adsorption capacities of both functionalized sepiolites at initial pH 5.0, when the equilibrium solution pH approached the value pH_{pzc}, indicates that the electrostatic interactions are not the only mechanism of adsorption, but also formation of hydrogen bonds between hydrogen from amine groups and oxygen from the dye and van der Waal's forces. The rate of adsorption is higher at lower pH values and at higher temperatures. The adsorption involves the intraparticle diffusion, but it is not the rate-controlling step.

The adsorption kinetics was fitted fairly well to the pseudo-second-order kinetic model.

An increase of the adsorption capacity with increasing temperature indicates the endothermic nature of the RO 16 adsorption onto studied amine silane functionalized sepiolites. The adsorption behavior in all cases was best described with the Sips isotherm. The values of the Sips equilibrium constant K_a confirmed that stronger bonds between dye anions and the adsorbents active sites were formed at lower pH values.

Acknowledgment

The authors would like to acknowledge the financial support of the Ministry of Education and Science of the Republic of Serbia (Project No. III 45019).

Symbols

- c_e — Concentration of RO 16 in solution at equilibrium, mg/dm^3
- c_f — Final concentration of RO 16 in solution, mg/dm^3
- c_i — Initial concentration of RO 16 in solution, mg/dm^3
- c_t — Concentration of RO 16 in solution after contact time t, mg/dm^3
- h — Initial adsorption rate, mg/(g min)
- k_1 — Rate constant of the pseudo-first-order adsorption, 1/min
- k_2 — Rate constant of the pseudo-second-order model, g/(mg min)
- K_a — Sips equilibrium constant, (dm^3/mg)$^n S$
- K_f — Freundlich constant related to the adsorption capacity, (mg/g)(dm^3/mg)$^{1/n}$
- K_L — Langmuir constant, dm^3/mg
- m — Mass of the adsorbent, g
- n — Adsorption intensity parameter
- n_S — Index of heterogeneity
- q_e — Amount of RO 16 adsorbed at equilibrium, mg/g
- q_m — Maximum adsorption capacity of the adsorbent, mg/g
- q_t — Amount of RO 16 adsorbed at time t, mg/g
- R^2 — Correlation coefficient
- T — Temperature, K
- t — Time, h
- V — Volume of RO 16 solution, dm^3

References

[1] M.A.M. Salleh, D.K. Mahmoud, W.A.W.A. Karim, A. Idris, Cationic and anionic dye adsorption by agricultural solid wastes: a comprehensive review, Desalination, 280 (2011) 1–13.
[2] M.T. Yagub, T.K. Sen, S. Afroze, H.M. Ang, Dye and its removal from aqueous solution by adsorption: a review, Adv. Colloid Interface Sci., 209 (2014) 172–184.
[3] V. Janaki, K. Vijayaraghavan, A.K. Ramasamy, K.-J. Lee, B.-T. Oh, S. Kamala-Kannan, Competitive adsorption of Reactive Orange 16 and Reactive Brilliant Blue R on polyaniline/bacterial extracellular polysaccharides composite—a novel eco-friendly polymer, J. Hazard. Mater., 241–242 (2012) 110–117.
[4] T. Robinson, G. McMullan, R. Marchant, P. Nigam, Remediation of dyes in textile effluent: a critical review on current treatment technologies with a proposed alternative, Bioresour. Technol., 77 (2001) 247–255.
[5] A. Geethakarthi, B.R. Phanikumar, Adsorption of reactive dyes from aqueous solutions by tannery sludge developed activated carbon: kinetic and equilibrium studies, Int. J. Environ. Sci. Technol., 8 (2011) 561–570.
[6] V.K. Gupta, Suhas, Application of low-cost adsorbents for dye removal – a review, J. Environ. Manage., 90 (2009) 2313–2342.
[7] J.C. Cardoso, G.G. Bessegato, M.V.B. Zanoni, Efficiency compar ison of ozonation, photolysis, photocatalysis and photoelectrocatalysis methods in real textile wastewater decolorization, Water Res., 98 (2016) 39–46.
[8] G. Boczkaj, A. Fernandes, Wastewater treatment by means of advanced oxidation processes at basic pH conditions: a review, Chem. Eng. J., 320 (2017) 608–633.
[9] R. Wang, R. Yang, B. Wang, W. Gao, Efficient degradation of Methylene Blue by the nano TiO_2-functionalized graphene oxide nanocomposite photocatalyst for wastewater treatment, Water Air Soil Pollut., 227 (2016) 1–9.
[10] V. Katheresan, J. Kansedo, S.Y. Lau, Efficiency of various recent wastewater dye removal methods: a review, J. Environ. Chem. Eng., 6 (2018) 4676–4697.
[11] R. Wang, R. Yang, Y. Zhang, A study of applying green glucose-reduced graphene oxide in advanced treatment of different dies, Desal. Wat. Treat., 70 (2017) 387–393.
[12] A. Kausar, M. Iqbal, A. Javed, K. Aftab, Z.-i-H. Nazli, H.N. Bhatti, S. Nouren, Dyes adsorption using clay and modified clay: a review, J. Mol. Liq., 256 (2018) 395–407.
[13] T. Ngulube, J.R. Gumbo, V. Masindi, A. Maity, An update on synthetic dyes adsorption onto clay based minerals: a state-of-art review, J. Environ. Manage., 191 (2017) 35–57.
[14] O. Duman, S. Tunç, T.G. Polat, Adsorptive removal of triarylmethane dye (Basic Red 9) from aqueous solution by sepiolite as effective and low-cost adsorbent, Microporous Mesoporous Mater., 210 (2015) 176–184.
[15] M. Doğan, Y. Özdemir, M. Alkan, Adsorption kinetics and mechanism of cationic methyl violet and methylene blue dyes onto sepiolite, Dyes Pigm., 75 (2007) 701–713.
[16] M. Doğan, M. Alkan, Ö. Demirbaş, Y. Özdemir, C. Özmetin, Adsorption kinetics of maxilon blue GRL onto sepiolite from aqueous solutions, Chem. Eng. J., 124 (2006) 89–101.
[17] Y. Özdemir, M. Doğan, M. Alkan, Adsorption of cationic dyes from aqueous solutions by sepiolite, Microporous Mesoporous Mater., 96 (2006) 419–427.
[18] B. Karagozoglu, M. Tasdemir, E. Demirbas, M. Kobya, The adsorption of basic dye (Astrazon Blue FGRL) from aqueous solutions onto sepiolite, fly ash and apricot shell activated carbon: kinetic and equilibrium studies, J. Hazard. Mater., 147 (2007) 297–306.
[19] M. Tekbaş, N. Bektaş, H.C. Yatmaz, Adsorption studies of aqueous basic dye solutions using sepiolite, Desalination, 249 (2009) 205–211.
[20] İ. Küncek, S. Şener, Adsorption of methylene blue onto sonicated sepiolite from aqueous solutions, Ultrason. Sonochem., 17 (2010) 250–257.
[21] F. Tümsek, Ö. Avcı, Investigation of kinetics and isotherm models for the Acid Orange 95 adsorption from aqueous solution onto natural minerals, J. Chem. Eng. Data, 58 (2013) 551–559.
[22] M. Alkan, Ö. Demirbaş, S. Çelikçapa, M. Doğan, Sorption of Acid Red 57 from aqueous solution onto sepiolite, J. Hazard. Mater., B116 (2004) 135–145.
[23] M. Alkan, S. Çelikçapa, Ö. Demirbaş, M. Doğan, Removal of Reactive Blue 221 and Acid Blue 62 anionic dyes from aqueous solutions by sepiolite, Dyes Pigm., 65 (2005) 251–259.
[24] M. Alkan, Ö. Demirbaş, M. Doğan, Adsorption kinetics and thermodynamics of an anionic dye onto sepiolite, Microporous Mesoporous Mater., 101 (2007) 388–396.
[25] D. Bingol, N. Tekin, M. Alkan, Brilliant Yellow dye adsorption onto sepiolite using a full factorial design, Appl. Clay Sci., 50 (2010) 315–321.
[26] O. Ozdemir, B. Armagan, M. Turan, M.S. Çelik, Comparison of the adsorption characteristics of azo-reactive dyes on mezoporous minerals, Dyes Pigm., 62 (2004) 49–60.
[27] A. Tabak, E. Eren, B. Afsin, B. Caglar, Determination of adsorptive properties of a Turkish Sepiolite for removal of

Reactive Blue 15 anionic dye from aqueous solutions, J. Hazard. Mater., 161 (2009) 1087–1094.
[28] M. Uğurlu, Adsorption of a textile dye onto activated sepiolite, Microporous Mesoporous Mater., 119 (2009) 276–283.
[29] S. Vahidhabanu, A.A. Idowu, D. Karuppasamy, B.R. Babu, M. Vineetha, Microwave initiated facile formation of sepiolite-poly(dimethylsiloxane) nanohybrid for effective removal of Congo Red dye from aqueous solution, ACS Sustainable Chem. Eng., 5 (2017) 10361–10370.
[30] A. Özcan, E.M. Öncü, A.S. Özcan, Adsorption of Acid Blue 193 from aqueous solutions onto DEDMA-sepiolite, J. Hazard. Mater., B129 (2006) 244–252.
[31] A. Özcan, A.S. Özcan, Adsorption of Acid Red 57 from aqueous solutions onto surfactant-modified sepiolite, J. Hazard. Mater., B125 (2005) 252–259.
[32] M.A. Moreira, K.J. Ciuffi, V. Rives, M.A. Vicente, R. Trujillano, A. Gil, S.A. Korili, E.H. de Faria, Effect of chemical modification of palygorskite and sepiolite by 3-aminopropyltriethoxisilane on adsorption of cationic and anionic dyes, Appl. Clay Sci., 135 (2017) 394–404.
[33] J. Zhang, Z. Yan, J. Ouyang, H. Yang, D. Chen, Highly dispersed sepiolite-based organic modified nanofibers for enhanced adsorption of Congo Red, Appl. Clay Sci., 157 (2018) 76–85.
[34] V. Marjanović, S. Lazarević, I. Janković-Častvan, B. Potkonjak, Đ. Janaćković, R. Petrović, Chromium (VI) removal from aqueous solutions using mercaptosilane functionalized sepiolites, Chem. Eng. J., 166 (2011) 198–206.
[35] V. Marjanović, S. Lazarević, I. Janković-Častvan, B. Jokić, Dj. Janaćković, R. Petrović, Adsorption of chromium(VI) from aqueous solutions onto amine-functionalized natural and acid-activated sepiolites, Appl. Clay Sci., 80–81 (2013) 202–210.
[36] S. Lazarević, I. Janković-Častvan, D. Jovanović, S. Milonjić, Dj. Janaćković, R. Petrović, Adsorption of Pb^{2+}, Cd^{2+} and Sr^{2+} ions onto natural and acid-activated sepiolites, Appl. Clay Sci., 37 (2007) 47–57.
[37] S. Lagergren, Zur theorie der sogenannten adsorption gelöester stoffe, K. Sven. Vetenskapsakad. Handl., 24 (1898) 1–39.
[38] G. Annadurai, M.R.V. Krishnan, Adsorption of acid dye from aqueous solution by chitin: equilibrium studies, Indian J. Chem. Technol., 4 (1997) 217–222.
[39] W.J. Weber, J.C. Morris, Kinetics of adsorption on carbon from solution, J. Sanitary Eng. Div., 89 (1963) 31–59.
[40] Y.S. Ho, G. McKay, Pseudo-second order model for sorption processes, Process Biochem., 34 (1999) 451–465.
[41] C. Su, W. Li, Y. Wang, Adsorption property of direct fast black onto acid-thermal modified sepiolite and optimization of adsorption conditions using Box-Behnken response surface methodology, Front. Environ. Sci. Eng., 7 (2013) 503–511.
[42] M.T. Mihajlović, S.S. Lazarević, I.M. Janković-Častvan, J. Kovač, B.M. Jokić, Dj.T. Janaćković, R.D. Petrović, Kinetics, thermodynamics, and structural investigations on the removal of Pb^{2+}, Cd^{2+}, and Zn^{2+} from multicomponent solutions onto natural and Fe(III)-modified zeolites, Clean Technol. Environ. Policy, 17 (2015) 407–419.
[43] A.A. Ahribesh, S. Lazarević, I. Janković-Častvan, B. Jokić, V. Spasojević, T. Radetić, Đ. Janaćković, R. Petrović, Influence of the synthesis parameters on the properties of the sepiolite-based magnetic adsorbents, Powder Technol., 305 (2017) 260–269.
[44] I. Langmuir, The adsorption of gases on plane surfaces of glass, mica and platinum, J. Am. Chem. Soc., 40 (1918) 1361–1403.
[45] K.Y. Foo, B.H. Hameed, Insights into the modeling of adsorption isotherm systems, Chem. Eng. J., 156 (2010) 2–10.
[46] H. Freundlich, Concerning adsorption in solutions, Z. Phys. Chem. Stoechiom. Verwandtschafts., 57 (1906) 385–470.
[47] V. Hernández-Montoya, M.A. Pérez-Cruz, D.I. Mendoza-Castillo, M.R. Moreno-Virgen, A. Bonilla-Petriciolet, Competitive adsorption of dyes and heavy metals on zeolitic structures, J. Environ. Manage., 116 (2013) 213–221.
[48] A.M. Sevim, R. Hojiyev, A. Gül, M.S. Çelik, An investigation of the kinetics and thermodynamics of the adsorption of a cationic cobalt porphyrazine onto sepiolite, Dyes Pigm., 88 (2011) 25–38.